Available online at www.sciencedirect.com
SCIENCE DIRECT®
Journal of Computational Physics 188 (2003) 56–74
JOURNAL OF COMPUTATIONAL PHYSICS
www.elsevier.com/locate/jcp

# Pseudospectral methods on a semi-infinite interval with application to the hydrogen atom: a comparison of the mapped Fourier-sine method with Laguerre series and rational Chebyshev expansions

John P. Boyd [a,*], C. Rangan [b], P.H. Bucksbaum [b]

[a] *Department of Atmospheric, Oceanic and Space Science, University of Michigan, 2455 Hayward Avenue, Ann Arbor, MI 48109-2143, USA*
[b] *Department of Physics, FOCUS Center, University of Michigan, Ann Arbor, MI 48109-1120, USA*

Received 16 August 2002; received in revised form 10 January 2003; accepted 7 February 2003

**Abstract**

The Fourier-sine-with-mapping pseudospectral algorithm of Fattal et al. [Phys. Rev. E 53 (1996) 1217] has been applied in several quantum physics problems. Here, we compare it with pseudospectral methods using Laguerre functions and rational Chebyshev functions. We show that Laguerre and Chebyshev expansions are better suited for solving problems in the interval $r \in [0, \infty]$ (for example, the Coulomb–Schrödinger equation), than the Fourier-sine-mapping scheme. All three methods give similar accuracy for the hydrogen atom when the scaling parameter $L$ is optimum, but the Laguerre and Chebyshev methods are less sensitive to variations in $L$. We introduce a new variant of rational Chebyshev functions which has a more uniform spacing of grid points for large $r$, and gives somewhat better results than the rational Chebyshev functions of Boyd [J. Comp. Phys. 70 (1987) 63].


*Keywords:* Eigenvalue; Semi-infinite interval; Mapped Fourier-sine method; Rational Chebyshev; Quantum mechanics; Coulomb; Laguerre

## 1. Introduction

Fattal et al. [19] introduced a pseudospectral method for quantum molecular dynamics which has been widely used. To discretize the radial coordinate $r$ of a spherical or cylindrical coordinate system, Fattal et al. employed a Fourier-sine series in combination with a change of coordinates (''mapping''). Radius $r$ is artificially extended to negative values so that the sine series converges to a function which is singular at the

* Corresponding author. Tel.: 1-734-764-3338; fax: 1-734-764-5137.
*E-mail address:* jpboyd@umich.edu (J.P. Boyd).

0021-9991/03/$ - see front matter © 2003 Elsevier Science B.V. All rights reserved.
doi:10.1016/S0021-9991(03)00127-X

origin. Even so, they show that their algorithm works well for two quantum eigenproblems: the bound states of the hydrogen atom and of the $H_2^+$ molecular ion.

In this article, we compare the Fourier-sine-mapping scheme with two alternatives. The Laguerre pseudospectral method employs collocation at the $N$ roots of the Laguerre function and approximates the wavefunction as a series of Laguerre functions. The rational Chebyshev method maps the interval $r \in [0, \infty]$ into $t \in [0, \pi]$ and then applies the Fourier cosine pseudospectral method. This is equivalent, with a different change-of-coordinate, to a basis of Chebyshev polynomials. The transformed cosines or Chebyshev polynomials are rational functions of $r$ (and of a square root factor of $r$), so we have dubbed this, in a mild abuse of notation, a "rational Chebyshev" basis.

In earlier work [9], we introduced a set of rational Chebyshev basis functions denoted by $\mathrm{TL}_j$. Although these basis functions work well for eigenproblems [9,18,22], the TL-grid has the disadvantage that points for large $r$ are not uniform, but rather the separation between adjacent grid points grows quadratically with $r$. As we show later in the paper, the eigenfunctions oscillate uniformly with radius, so the non-uniform TL-grid is disadvantageous. In this article, we introduce a new series of related functions $\mathrm{TM}_j$ which define a more uniform grid for large $r$. We show that these give better results than the TL functions for the Coulomb problem.

## 2. The pseudospectral method for eigenproblems

To solve a differential eigenproblem

$$a_2(r)u_{rr} + a_1(r)u_r + a_0(r)u = \lambda b(r)u, \tag{1}$$

the first step for any of the basis sets described here is to expand $u$ as a series, truncated after the $N$th term:

$$u(r) = \sum_{j=1}^{N} u_j \phi_j(r). \tag{2}$$

The pseudospectral method, also known as "collocation", "discrete ordinates" [24], and "selected points", demands that when the series is substituted into the differential equation, the residual is zero at each of $N$ "collocation" points. This is equivalent to the generalized matrix eigenproblem

$$\vec{\boldsymbol{A}}\vec{\boldsymbol{u}} = \lambda \vec{\boldsymbol{B}}\vec{\boldsymbol{u}}, \tag{3}$$

where $\vec{\boldsymbol{u}}$ is a column vector containing the spectral coefficients and where the elements of the matrices are given by

$$A_{ij} = a_2(r_i)\phi_{j,rr}(r_i) + a_1(r_i)\phi_{j,r}(r_i) + a_0(r_i)\phi_j(r_i), \quad B_{ij} = b(r_i)\phi_j(r_i). \tag{4}$$

Every basis set has a canonical choice of collocation points $r_i$. Pseudospectral treatment of eigenproblems is reviewed in Chapter 7 of [14]. Only some of the matrix eigenvalues are good approximations to those of the differential equation (typically about $N/2$). It is always necessary (except for test problems!) to redo the calculation with different $N$ to determine which eigenvalues are trustworthy [6,13,14].

## 3. The hydrogen atom

The energy levels of the hydrogen atom are the eigenvalues $E$ of

$$-\frac{1}{2}u_{rr} + \left(\frac{\ell(\ell+1)}{2r^2} - \frac{1}{r}\right)u = Eu, \quad r \in [0, \infty], \tag{5}$$

where the eigenvalues are

$$E_n = -\frac{1}{2n^2}, \quad n = 1, 2, \ldots \tag{6}$$

with eigenfunctions

$$u_{n,\ell} = r\exp(-r/n)\,(2r/n)^{\ell} L_{n+\ell}^{2\ell+1}(2r/n), \quad n \geqslant \ell + 1, \tag{7}$$

where $L_n^m$ is the usual generalized Laguerre polynomial [1]. Here $r$ is the radial coordinate in a spherical coordinate system. $\ell$ is the angular momentum quantum number.

One might suppose that this problem would be difficult because of the $1/r$ and $1/r^2$ terms in the coefficient of the undifferentiated term. In reality, none of the pseudospectral methods has any difficulty at $r = 0$ because of the unbounded coefficients. One might further suppose that it would be necessary to explicitly impose boundary conditions at $r = 0$ and $r = \infty$. In reality, none of the pseudospectral methods needs to explicitly impose boundary conditions. The analytic basis functions automatically converge to whatever solution is bounded at both $r = 0$ and $r = \infty$ in spite of the fact that the differential equation is singular at both endpoints. This is not true only of the hydrogen atom, but of differential equations on a semi-infinite ($r \in [0, \infty]$) interval in general [7,14].

The major numerical challenge is rather that the eigenmodes are functions of $r/n$. This implies that there is no single choice of a width for the basis functions which is optimum for all modes.

## 4. The mapped Fourier-sine method of Fattal, Baer and Kosloff (1996)

Fattal, Baer and Kosloff expanded $u$ as a series of transformed sine functions of the form

$$\phi_j(r) \equiv \sin\left(j\frac{\pi}{L}x(r)\right), \tag{8}$$

where $x(r)$ is given by the inverse of a mapping function of the form

$$r = f(x) \tag{9}$$

and where the computational coordinate $x \in [-L, L]$ for some domain truncation parameter $L$. The Fourier series is periodic in $x$ in the sense that $u(x + P) = u(x)$ for all $x$, where the period $P = 2L$.

The mapping is needed because Fattal et al. chose a Fourier basis so that the matrix elements could be constructed by using the Fast Fourier Transform (FFT). The merits and flaws of the FFT are discussed later; the immediate issue is: How can one apply a basis composed of periodic functions to approximate functions which are not periodic?

Fattal et al.'s answer was to extend the radial coordinate to negative values in such a way that $u$ decays exponentially fast as $|r| \to \infty$. If the spatial period $2L$ is sufficiently large, then $u(\pm L)$ is negligibly small. The errors in a Fourier series due to lack of periodicity will then be exponentially small in $L$ [11]. To avoid the waste of collocation points at negative $r$, Fattal et al. restrict the Fourier basis to a *sine* series which implies that the approximation $u_N$ is an *antisymmetric* function with respect to $r$ in the sense that $u_N(-r) = -u_N(r)$ for all $r$. It is then sufficient to use collocation points only for $r_j > 0$ since the collocation conditions for negative $r$ would just be the negative of the conditions for $r > 0$. The mapping function is chosen to be an antisymmetric function so that $u_N(r(x))$ is antisymmetric in the computational coordinate $x$ as well as in the physical coordinate $r$.

One minor restriction is that a sine series is always zero at $x = 0$. Therefore, the mapped sine method is only applicable when $u(r)$ satisfies the boundary condition $u(0) = 0$. (The Laguerre and rational Chebyshev methods impose no such restrictions.)

A far more serious problem is that the ground state of the hydrogen atom has the analytic form

$$u_{0,0} = r\exp(-r). \tag{10}$$

Because all the sine functions are individually antisymmetric in both $x$ and $r$, it follows that a Fourier series that converges to $r\exp(-r)$ for $r > 0$ must converge over the whole interval to

$$\tilde{u}_{0,0} \equiv r\exp(-|r|) \tag{11}$$

since this is the unique function which is defined for positive $r$ as the hydrogen ground state, and for negative $r$ by the antisymmetry condition $\tilde{u}_{0,0}(-r) \equiv -\tilde{u}_{0,0}(r)$.

Thus, the antisymmetric extension has converted an infinitely differentiable function which is analytic for all real $r$ into a function which has a discontinuous second derivative at the origin! The price paid for this can be found by writing down the usual coefficient integral,

$$b_n \equiv \frac{2}{L}\int_0^L \sin\left(n\frac{\pi}{L}x\right)u(x)\,\mathrm{d}x. \tag{12}$$

Integrating by parts three times, and noting that the integrand $u(x)$ is an analytic function – it is singular only when extended antisymmetrically *outside* the integration range to negative $x$ – we find

$$b_n \sim -\frac{2L^2}{n^3\pi^3}u_{xx}(0) + \mathrm{O}(1/n^5), \quad n \to \infty. \tag{13}$$

Thus, the usual geometric convergence of the Fourier series of a periodic, analytic function (i.e., $b_n \sim p\exp(-qn)$), where $p$ and $q > 0$ are constants) has been replaced by a third-order algebraic rate of convergence with $b_n \sim \mathrm{O}(1/n^3)$. When the series is summed, one loses a power of $n$ (p. 51 of [14]) so that, defining $N$ as the truncation of the Fourier series, the maximum pointwise error in $u_N$ decreases only as $\mathrm{O}(1/N^2)$; empirically, Fattal et al. (p. 1222) show that the same is true of the eigenvalue error.

The second derivative of $u$ with respect to the computational coordinate is controlled by the mapping:

$$u_{xx}(0) = (f_x(0))^2 u_{rr}(r = 0), \tag{14}$$

where we have assumed that the mapping function $r = f(x)$ is antisymmetric in $x$, which implies that all its even derivatives are zero at the origin. It follows that by making a change-of-coordinate, the effect of the singularity at $r = 0$ can be made arbitrarily weak by choosing the mapping so that $f_x(0)$ is very small. Since the optimum Fourier grid is evenly spaced in $x$, it follows that such a mapping will cluster grid points very densely near the origin, exactly what one would expect would be needed to resolve a singularity at $r = 0$.

Fattal et al.'s own choice of mapping is

$$r = x - A\arctan(\beta x) = f(x), \tag{15}$$

where $A$ and $\beta$ are constants. Derivatives of the basis functions with respect to $r$ can be evaluated from the $x$-derivatives by applying the chain rule repeatedly:

$$\frac{\mathrm{d}\phi_j}{\mathrm{d}r} = \frac{1}{\mathrm{d}f/\mathrm{d}x}\frac{\mathrm{d}\phi_j}{\mathrm{d}x} = \frac{1}{\mathrm{d}f/\mathrm{d}x}\,j\cos(jx(r)), \tag{16}$$

$$\frac{d^2\phi_j}{dr^2} = \frac{1}{(df/dx)^2}\frac{d^2\phi_j}{dx^2} - \frac{d^2f/dx^2}{(df/dx)^3}\frac{d\phi_j}{dx}, \tag{17}$$

where for Fattal et al.'s own map, explicit differentiation gives

$$\frac{df}{dx} = 1 - \frac{A\beta}{1+\beta^2x^2}, \quad \frac{d^2f}{dx^2} = 2\frac{A\beta^3x}{\left(1+\beta^2x^2\right)^2}. \tag{18}$$

Among the many later applications of this method, Borisov [5], Lemoine [21], and Nest and Meyer [23] have tweaked the mapped sine method by applying different changes of coordinate. However, the (weakened) singularity at the origin remains.

Fig. 1 shows the isolines of the number of accurate eigenvalues in the $L$–$N$ plane where the horizontal axis is the domain size in the computational coordinate and $N$ is the number of grid points (and also the number of basis functions). The heavy dashed line shows that the optimum $L$ increases linearly with $N$. It is a generic property of infinite interval spectral methods that the best choice of domain size or scaling parameter is $N$-dependent [2,3,8–10,15,16,25]. It is possible to obtain as many as 37 "good" eigenvalues with only 60 grid points. This impressive performance has inspired very wide use of the mapped Fourier method.

However, the contour plot also illustrates some of the flaws of the mapped sine Fourier method. Above the dashed line which connects the best values of $L$ for each $N$, the contour lines are vertical. The reason is that the mapped sine Fourier algorithm is a "domain truncation" method. That is, the algorithm is accurate only for eigenmodes which decay to negligible values at $x = \pm L$. Since the modes of the hydrogen atom decay more and more slowly as the mode number $n$ increases, it follows that only a finite number of eigenvalues can be accurately approximated for a given fixed domain size $L$. The contour lines become vertical because once $N$ is large enough to resolve all the modes that decay on a domain of size $L$, increasing $N$ still further is useless.

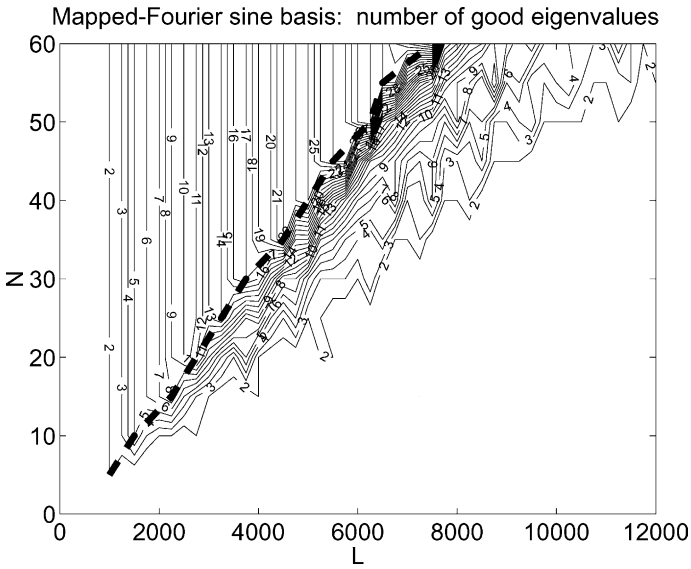


Fig. 1. The isolines of the number of accurate eigenvalues in $L$–$N$ plane as computed by collocation using the Fattal–Baer–Kosloff. A "good" eigenvalue is defined as one for which the difference between $1/E_{\text{numerical}}(n)$ and $-2n^2$ is smaller than 1/2. The heavy dashed line connects the points which, for a given $N$, have the maximum number of "good" eigenvalues as $L$ varies. With $L = L_{\text{optimum}}(N)$ as defined by this dashed line, the number of good eigenvalues is $N/2$ or more.

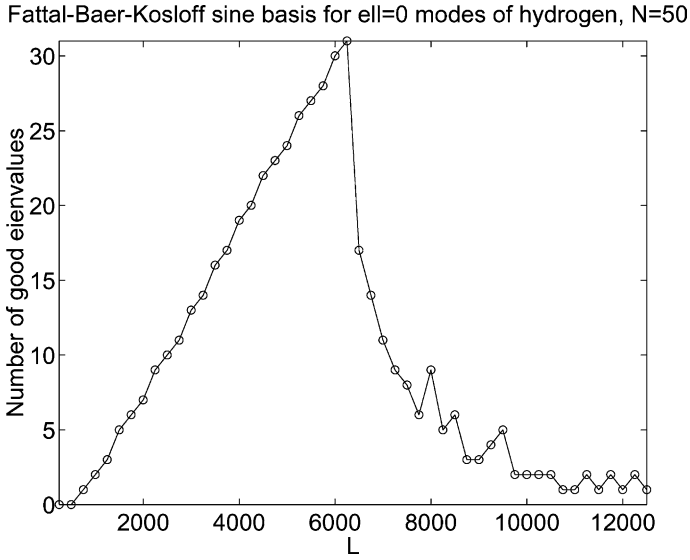


Fig. 2. A comparison of the number of accurate eigenvalues versus domain size $L$ for $N = 50$ sine functions. A "good" eigenvalue is defined as one for which the difference between $1/E_{\text{numerical}}(n)$ and $-2n^2$ is smaller than 1/2. The maximum number of good eigenvalues is 31 for $L = 6250$.

The contour plot also shows that there is a rather narrow domain in the $L$–$N$ plane which yields a lot of accurate eigenvalues. Fig. 2, which shows the number of accurate eigenvalues versus domain size $L$, makes the same point more clearly. The mapped Fourier method can yield as many as 31 accurate eigenvalues for $N = 50$ grid points, but the number of "good" eigenvalues falls off very steeply as $L$ increases above $L_{\text{optimum}}(N)$, and decreases less steeply but still rapidly when $L$ decreases below $L_{\text{optimum}}(N)$.

The reason, as explained for a different unbounded interval domain truncation method in [8], is that the total error is the sum of two contributions: a domain truncation error $E_{\text{D}}(L)$ which depends only on the domain size (and is roughly $|u(x = L)|/\max|u|$) plus a series truncation error $E_{\text{S}}(L, N)$. For fixed $N$, these two contributions vary oppositely with $L$: the domain truncation error $E_{\text{D}}$ decreases with $L$ (since the eigenmode at the boundary, $|u(L)|$, is decreasing exponentially fast with $L$) while the series error $E_{\text{S}}(L, N)$ *grows* with domain size since a given number of spectral functions are being asked to approximation $u(r)$ on a larger interval. The sharply pointed peak in Fig. 1 is the result of the competition between these two tendencies.

In contrast, the two competing methods described below are not methods of domain truncation, but instead approximate $u$ over the entire semi-infinite interval. The total error is therefore the series truncation error $E_{\text{S}}(L, N)$. Because this is an analytic function of $L$, the error curve and also the number of good eigenvalues versus $L$ for fixed $N$ are both *flat*, i.e., have zero derivative with respect to $L$, in the vicinity of $L = L_{\text{optimum}}(N)$. The practical consequence is that the competing Laguerre and rational Chebyshev series are significantly *less sensitive* to $L$ than the rational Fourier method. One therefore does not need to do as much experimentation to find an optimum $L$.

## 5. Usefulness of the fast Fourier transform

In [5,19,21], much is made of the efficiency of evaluating matrix elements through multiple applications of the Fast Fourier Transform (FFT). For time-dependent problems where the action of a differential

operator on a function may need to be evaluated a hundred thousand times (if that is the number of time steps), the FFT is indeed very useful. For eigenproblems, however, the FFT does not improve efficiency unless the eigenvalues are computed one at a time through a preconditioned iteration.

The reason is that the standard algorithm for eigenproblems, the QR/QZ method, has a cost which is roughly $10N^3$ operations where $N$ is the size of the matrix. The cost of computing the matrix elements by the direct formulas illustrated above scales only as $O(N^2)$ which – given that the pseudospectral matrices are *dense* with $N^2$ nonzero elements – is the best one can hope to do. The cost of forming the elements is always negligible compared to the expense of the QR/QZ algorithm; even for $N = 32$, the operation count for forming the matrix elements is 60 times smaller than the operation count for the QZ method.

In contrast, the FFT is very useful for time-dependent problems. When the time-marching scheme is explicit, it is unnecessary to compute the eigenvalues of a matrix or even to factor a matrix. Instead, it is merely necessary to apply a differential operator to the solution. Through the FFT, this operator can be evaluated at a cost, with $N$ degrees of freedom in each dimension, which is $O(\log_2(N))$ larger than the total number of degrees of freedom. Since our focus here is limited to eigenproblems, we refer to Chapter 9 of [14] for details.

## 6. Laguerre eigensolver

To demonstrate the use of symmetry-suited basis functions in pseudospectral methods, we solved the hydrogen atom eigenproblem using a Laguerre series in the form

$$u(r) = \sum_{j=0}^{N-1} a_j \phi_j(r/L), \tag{19}$$

$$\phi_j(r) \equiv \exp(-r/2) L_j(r), \quad j = 0, 1, 2, \ldots, N-1, \tag{20}$$

where $L > 0$ is the scaling parameter and $L_j$ is the Laguerre polynomial of degree $j$. (Note that "$L$" with a *numerical* subscript will always denote Laguerre polynomials whereas "$L$" without a subscript or with a multiletter subscript will always denote the "map parameter" or "stretching factor".) The collocation points are $r_i = L\rho_i, i = 0, 1, \ldots, (N-1)$ where the set of $\rho_i$ are the roots of $L_N(x)$. These can be can be computed in Matlab by the pair of statements **J = diag ([1:2:2*N-1])-diag([1:N-1],1)-diag([1:N-1],-1); r = sort(eig(sparse(J)));** [26], or in Maple by **with(orthopoly); fsolve(L(N,x),x)** or by consulting the tables in [17]. The basis functions themselves and all needed derivatives can be computed by using the identity $d^m L_n/dx^m = (-1)^m L_n^{(m)}$ where the generalized Laguerre polynomials (with $L_n \equiv L_n^0$) are given by

$$L_0^{(m)} \equiv 1, \quad L_1^{(m)} \equiv 1 + m - x, \quad L_{n+1}^{(m+1)} = \frac{(2n+m+1)-x}{n+1} L_n^{(m)} - \frac{n+m}{n+1} L_{n-1}^{(m)}. \tag{21}$$

Fig. 3 shows that the Laguerre pseudospectral method is very accurate. As for the other methods, no one choice of the scale parameter $L$ is best for all modes: small $n$ modes are most accurately approximated by small $L$ while larger modes are wider and wider, and require larger and larger $L$. Unlike the Fourier-sine-mapped method, the Laguerre expansion does not require that $u(0) = 0$.

Fig. 3 shows that the hydrogen atom is a very wierd eigenvalue problem. A typical non-quantum eigenproblem is $u_{xx} + \lambda u = 0,\ u(0) = u(\pi) = 0$, which has the exact eigenfunctions $u_n = \sin(nx), \lambda_n = n^2$. For this, the eigenfunctions oscillate more and more rapidly as the mode number $n$ increases. A pseudospectral method with a given truncation $N$ will therefore approximate the eigenvalues with an accuracy that is greatest for the very lowest mode and then decreases rapidly as the mode number $n$ increases. For the hydrogen atom, in contrast, a large value of the scaling parameter $L$ creates a Laguerre expansion which is

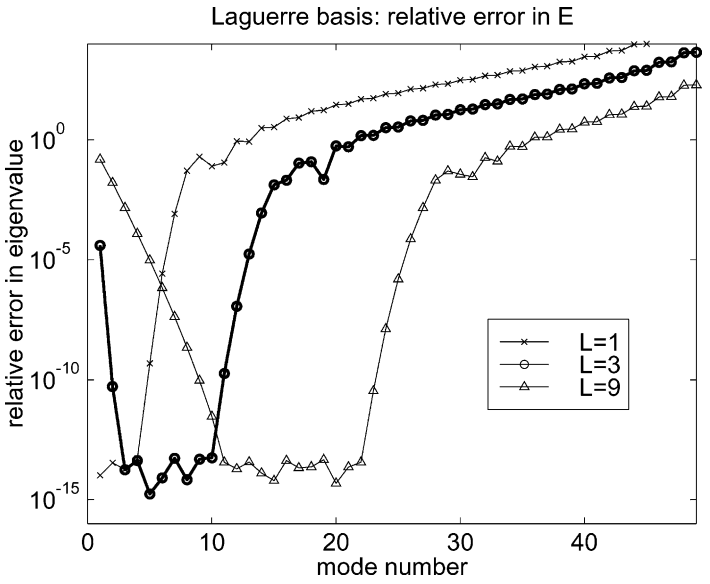


Fig. 3. Laguerre basis: relative errors in the eigenvalues of the hydrogen atom ($\ell = 0$) for three different scaling parameters: $L = 1$, $L = 3$ (thick curve) and $L = 9$. $N = 50$ grid points. The relative error is defined as $|E_n - [-1/(2n^2)]|/[1/(2n^2)]$ where $n$ is the mode number.

most accurate for modes of *moderate* $N$ while the accuracy is poor or non-existent for both small $n$ and large $n$ modes. (The same is true for the Fourier mapped sine and rational Chebyshev methods, too, (not shown).) This behavior can be understood by looking at the wavefunctions of the hydrogen atom [20], whose average radial extents $\langle r_n \rangle$ scale as the square of the principal quantum number $n$ (equal to the mode number + the angular momentum quantum number $\ell$). By changing the scaling parameter $L$, which maps the physical space onto the collocation grid, we choose the spatial region (and hence mode number) that is best represented by the expansion functions. Comparing Eqs. (7) and (20), we can expect that a scaling parameter $L$ will best represent eigenfunctions with principal quantum numbers around $2L$, and this is seen in Fig. 3. Thus, $L$ can be used as a tuning parameter to accurately extract the eigenvalues and eigenfunctions of a range of eigenmodes. This feature can be exploited in several quantum problems (for example, Rydberg atoms), where the dynamics of the system involve a range of high eigenmodes, and the lower modes do not contribute.

## 7. Rational Chebyshev functions: an FFT-able basis for the semi-infinite interval

Fifteen years ago, the first author introduced a basis for problems on $r \in [0, \infty]$ which does not require extension to negative $r$ or the introduction of a spurious singularity at $r = 0$ but does, like the mapped Fourier-sine method, allow free use of the Fast Fourier Transform [9]. These functions, denoted $\mathrm{TL}_j$, have been successful in a range of applications [9,14,18,22]. They were defined in close analogy with similar functions for the unbounded interval [10], but have a disadvantage not shared by their infinite interval counterparts: the span of the *TL* grid points grows *quadratically* with $N$, that is, the largest grid point is $r_N \sim (16/\pi^2)LN^2$. When we found that the *TL* results were not quite as good as the Laguerre basis or the mapped Fourier-sine method, we therefore decided to experiment with a new set of rational Chebyshev functions for the semi-infinite interval:

$$\mathrm{TM}_j(r;L) \equiv \cos(jx(r)), \quad r = L\cot(x/2)\cos(x/2), \quad x \in [0,\pi][\text{“TM map”}], \tag{22}$$

With this map,

$$r \sim 2L/x, \quad x \ll 1, \tag{23}$$

which is the desired inverse-linear behavior; the largest grid point is at $r_N = (\pi/4)LN$. The basis functions can be alternatively written as

$$\mathrm{TM}_j(r;L) \equiv T_j\left(\frac{r\sqrt{r^2+16L^2}-(r^2+4L^2)}{4L^2}\right), \tag{24}$$

where the $T_j$ are the usual Chebyshev polynomials. It would be more accurate to say that these functions $\mathrm{TM}_j$ are ''rational-with-a-square-root factor Chebyshev polynomials'', but for brevity we shall call them ''rational Chebyshev'' even though they are not, strictly speaking, rational functions of $r$. The grid points are

$$r_j \equiv L\cot(x_j/2)\cos(x_j/2), \quad x_j \equiv (2j-1)/(2N), \quad j = 1,2,\ldots,N. \tag{25}$$

Derivatives of the basis functions with respect to $r$ can be evaluated from the $x$-derivatives by applying the chain rule repeatedly:

$$\frac{\mathrm{d}\phi_j}{\mathrm{d}r} = \frac{1}{\mathrm{d}r/\mathrm{d}x}\frac{\mathrm{d}\phi_j}{\mathrm{d}x} = \frac{1}{\mathrm{d}r/\mathrm{d}x}\, j\cos(jx(r)), \tag{26}$$

$$\frac{\mathrm{d}^2\phi_j}{\mathrm{d}r^2} = \frac{1}{(\mathrm{d}r/\mathrm{d}x)^2}\frac{\mathrm{d}^2\phi_j}{\mathrm{d}x^2} - \frac{\mathrm{d}^2r/\mathrm{d}x^2}{(\mathrm{d}r/\mathrm{d}x)^3}\frac{\mathrm{d}\phi_j}{\mathrm{d}x}, \tag{27}$$

$$\frac{\mathrm{d}r}{\mathrm{d}x} = \frac{L}{2}\cos(x/2)(\cos^2(x/2)-2)/\sin^2(x/2), \tag{28}$$

$$\frac{\mathrm{d}^2r}{\mathrm{d}x^2} = \frac{L}{4}\left\{2-\cos^2(x/2)+\cos^4(x/2)\right\}/\sin^3(x/2). \tag{29}$$

For $u(r)$, this basis is equivalent to expanding $\tilde{u}(x) \equiv u(r(x))$ as a cosine series in $x$. The mapping can be equivalently written as

$$r = \frac{L}{\sqrt{2}}\frac{1+\cos(x)}{\sqrt{1-\cos(x)}} \tag{30}$$

which shows explicitly that any function $u(r)$ will be transformed into a function of $\cos(x)$, and thereby automatically made into a periodic function in $x$. It is not necessary to employ domain truncation – the TM mapping transforms the entire interval $r \in [0,\infty]$ into $x \in [0,\pi]$. It is also unnecessary to introduce an artificial singularity at $r = 0$, and thus be forced to have a very high density of grid points in the neighborhood of $r = 0$, as with the mapped Fourier sine method.

The TM mapping has a square-root singularity at $x = 0 \leftrightarrow r = \infty$, but if $u(r)$ decays exponentially as $r \to \infty$, then the exponential decay wipes out the singularity in $\tilde{u}(x)$, and there is never a problem. If $u(r)$ has an asymptotic expansion in inverse powers of $r$ as $r \to \infty$, then convergence will be poor unless the series involves only even powers of $r$. However, the ability to handle some classes of functions with an algebraic rather than exponential decay as $r \to \infty$ is a generic advantage of rational basis functions over the mapped Fourier sines, which are restricted to exponentially decaying functions.

The TM grid is non-uniform, and like the Chebyshev polynomials, the TM grid points near $r = 0$ [$x = \pi$] have a spacing which is inverse quadratic, that is, nearest neighbors are separated by $O(1/N^2)$. However, this is much less dense than that of the mapped Fourier-sine method – one might describe the mapped Fourier-sine distribution of points as a "hyper-Chebyshev" grid.

Fig. 4 shows that the TM basis is indeed superior to the older TL basis for computing bound states of the hydrogen atom. We therefore use only TM functions for the comparisons given later with the mapped Fourier-sine and Laguerre methods.

To tweak the computations in Fig. 4 and exploit the fact that $u(0) = 0$ for this problem, we built this boundary condition into the basis functions by defining

$$\phi_j(r) \equiv \mathrm{TM}_j(r;L) - (-1)^j, \quad j = 1, 2, \ldots \tag{31}$$

so that $\phi_j(0) = 0$ for all $j$. This increased the number of accurate eigenvalues only by one compared to using $\phi_j \equiv \mathrm{TM}_{j-1}(r;L)$ as we confirmed by direct experiments, but it illustrates the flexibility inherent in the TM and TL functions.

To illustrate the simplicity of the pseudospectral method (without the unnecessary FFT transformations of [5,19,21]), Table 1 shows the complete Matlab program for solving the hydrogen atom through a TM basis. There are only 31 executable statements.

Although the Fast Fourier Transform is irrelevant for solving eigenproblems, the TM basis is just a Fourier cosine series in disguise. It goes almost without saying that when the TM basis is used to discretize the radial coordinate in a time-dependent calculation, the Fast Fourier Transform – more precisely, a fast cosine transform – can be used to evaluate all derivatives and operators.

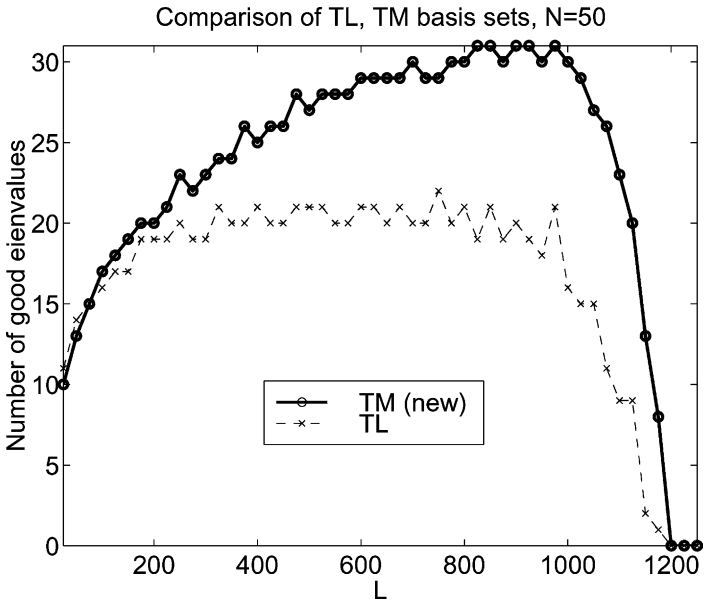


Fig. 4. The number of "good" eigenvalues for the $\ell = 0$ bound states of the hydrogen atom as computed by the older TL basis (bottom, thin curve) and the TM basis introduced here (top, thick).

Table 1
Eigensolver with TM basis for hydrogen bound states

```
el=0;  % angular number $\el$ for the hydrogen atom
L=100, % map parameter for basis functions
N=50,  % number of collocation points and basis functions
% For clarity, for/end loops have been displayed explicitly. However,
% Matlab/FORTRAN 90 code is more efficient if loops are vectorized
h=pi/N; xa=h/2:h:(pi-h/2); % ta: grid points in trigonometric argument t
for ii=1:N,  x=xa(ii);  S = sin(x/2);   C = cos(x/2);  ra(ii)=L* C*C/S;
for j=1:N,   cj=cos(j*x);   sj=sin(j*x);
phi_x = - j * sj;   phi_xx = -j*j*cj;  % x-derivatives of j-th basis func.
fx=0.5*L*C*(C*C-2)/(S*S);   % f1=dr/dx
fxx= 0.25*L*(2-C*C + C*C*C*C)/(S*S*S); % 2d derivative of r  w. r. t.  x
phi(ii,j)=(cj-cos(j*pi));   %  phi_j(r_i)
phir(ii,j)=phi_x/ fx;    %  d phi_j/dr(r_i)
phirr(ii,j)=(phi_xx - (fxx/fx)*phi_x )/(fx*fx);   % d**2 phi_j/dr**2(r_i)
end, end
% Assemble the matrices of the matrix eigenproblem, A*u = lambda*B*u
for ii=1:N,  r=ra(ii);  % ODE coefficients defined by next line
a2=-1/2;  a1=0;  a0=-1/r + el*(el+1)/(2*r*r);  b= 1;
for j=1:N,    A(ii,j) =  a2*phirr(ii,j) + a1*phir(ii,j) + a0*phi(ii,j);
B(ii,j) =  b* phi(ii,j);      end, end
[EIGFUNCTIONS,EIGVALS]=eig(A,B);    % solve matrix eigenproblems
[lambda,index]=sort(real(diag(EIGVALS))); % sort eigenvals.: smallest first
```

## 8. Comparisons between mapped Fourier-sine, Laguerre and rational Chebyshev basis sets

Fig. 5 compares the number of accurate eigenvalues for the three basis functions for $N = 50$. All three methods do well. There is little to choose between them when the map or scale parameter is equal to its optimum value for a given method. However, it is obvious that the mapped Fourier-sine method loses accuracy much more rapidly than the other schemes as $L$ varies away from its optimum value.

Since the optimum $L$ varies with $N$, some experimentation is needed to pick a good $L$ for a given problem and resolution. Clearly, more experimentation is required for the mapped Fourier-sine method.

Fig. 6 shows the relative errors in the eigenvalues and the maximum pointwise relative errors in the eigenfunctions obtained by using the optimum $L$ for $N = 50$ for the three basis functions. Even though the optimum $L$ value for each basis function produces the same *number* of good eigenvalues, the errors in the eigenvalues and eigenvectors differ by orders of magnitude depending on the chosen basis. In quantum physics problems such as the calculation of oscillator strengths or the dynamics of a superposition of several eigenstates, it is very important to have low errors in eigenfunctions. The Laguerre basis functions give the best eigenfunctions and eigenvalues for a range of eigenmodes.

### 8.1. Lithium

As a second example, we calculate the energies and radial wavefunctions of lithium, an atom with one valence electron. The potential due to the nucleus and the two inner-shell electrons does not have an

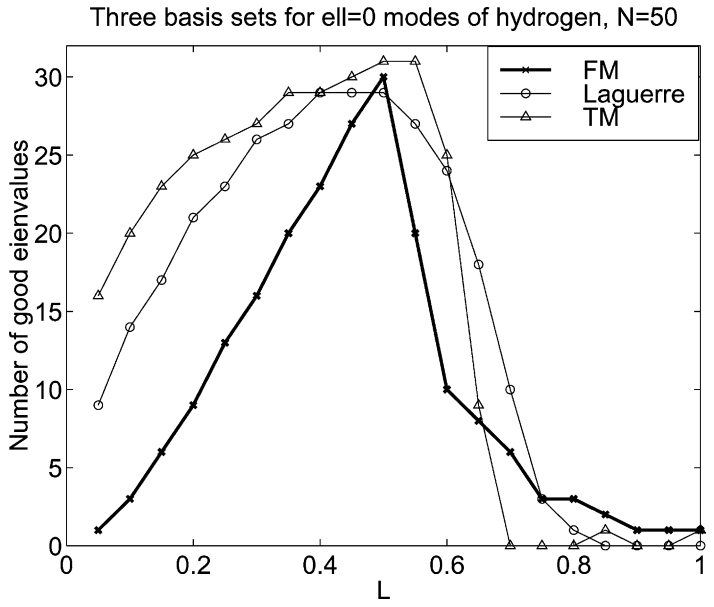


Fig. 5. The number of accurate eigenvalues versus $L$ for $N = 50$ as computed by collocation using three different methods. The map parameter/scaling parameter/domain size $L$ has been scaled by roughly $2L_{\text{optimum}}$ for each method so that the three curves are aligned. A "good" eigenvalue is defined as one for which the difference between $1/E_{\text{numerical}}(n)$ and $-2n^2$ is smaller than 1/2.

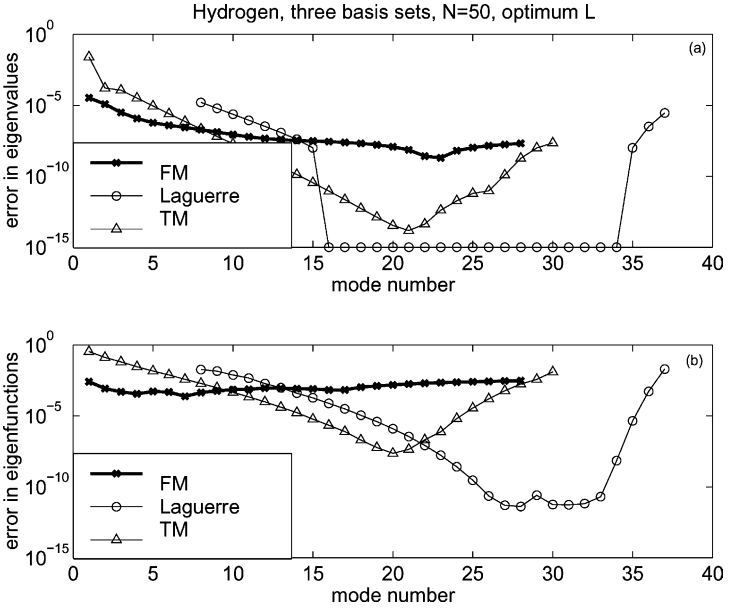


Fig. 6. The errors in the eigenvalues (a) and the maximum relative errors in the eigenvectors (b) versus mode number for $N = 50$ and optimum $L$ as computed by collocation using three different methods. Points are shown only for the "good" eigenvalues calculated as described in the previous figure.

analytic form, but can be represented by a pseudopotential [4] which is dependent on the angular momentum $\ell$. The Schrödinger equation for lithium is:

$$-\frac{1}{2}u_{rr}+\left\{A_\ell \exp(-Si_\ell)-\frac{0.1925+0.112/(r^2+9/16)}{2(r^2+9/16)^2}+\frac{\ell(\ell+1)}{2r^2}-\frac{1}{r}\right\}u=Eu \tag{32}$$

with $A_0=6.013668,\ Si_0=1.293213,\ A_1=-0.740679,\ Si_1=1.410279$ and $A_\ell=-0.067342,\ Si_\ell=0.8$ for all $\ell>1$ and where the eigenvalues are *approximately*

$$E_n=-\frac{1}{2}\frac{1}{(n-q(\ell))^2},\quad n=1,2,\ldots, \tag{33}$$

where $q(0)=0.399,\ q(1)=0.053,\ q(2)=0.002$ and $q(\ell)=0$ if $\ell>2$.

Fig. 7 shows the number of accurate eigenvalues calculated for angular momentum $\ell=0$, 1, and 12, respectively. For contrast, we used a larger number of collocation points (100) and a stricter criterion of

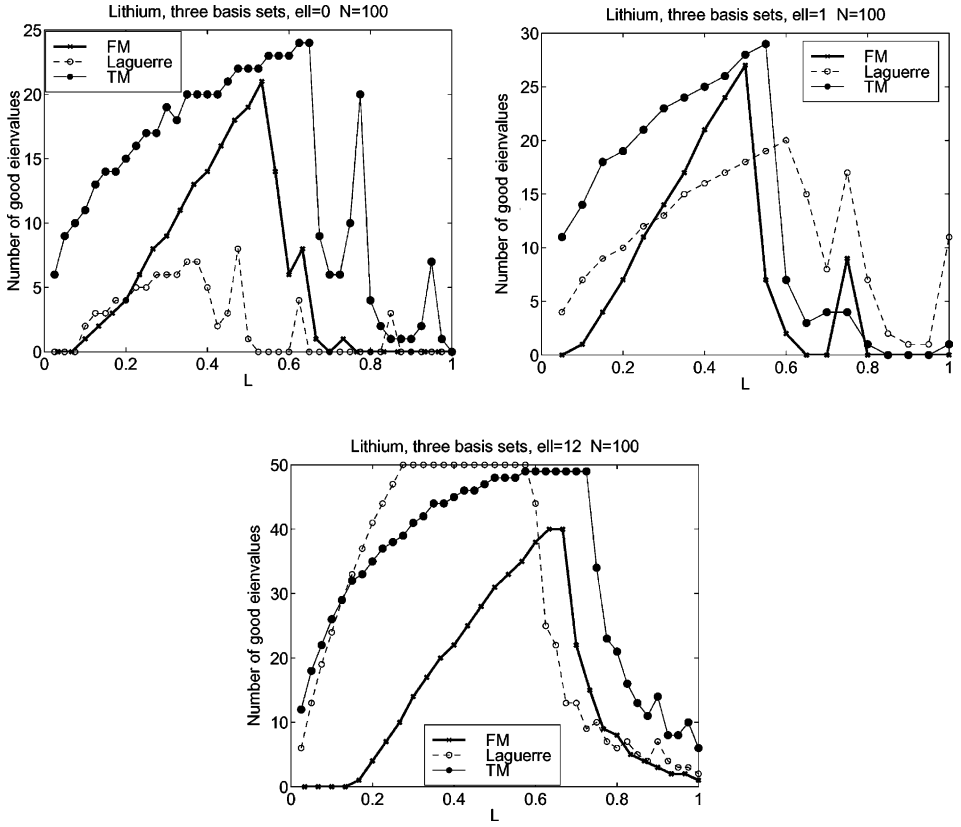


Fig. 7. The number of accurate eigenvalues versus $L/L_{\max}$ with $N=100$ collocation points using three different methods. (a) $\ell=0$: The maximum map or scale parameters for each method are $L_{\max}(\text{FourierMapped})=9000$, $L_{\max}(\text{Laguerre})=5$, and $L_{\max}(\text{TM})=320$. (b) $\ell=1$: $L_{\max}(\text{FourierMapped})=12000$, $L_{\max}(\text{Laguerre})=5$, and $L_{\max}(\text{TM})=600$. (c) $\ell=12$: $L_{\max}(\text{FM})=18000$, $L_{\max}(\text{Laguerre})=80$ and $L_{\max}(\text{rational Chebyshev})=6400$. A more stringent criterion for a "good" eigenvalue was used than for hydrogen: $|1/\lambda_{\text{exact}}-1/\lambda_{\text{numerical}}|<1/1000$.

"goodness", $|1/\lambda_{\text{exact}} - 1/\lambda_{\text{numerical}}| < 1/1000$, than for hydrogen. (The "exact" lithium eigenvalues are those numerically calculated with very large $N$.)

For all three $\ell$, the rational Chebyshev method gives as many or more good eigenvalues as the Fourier-mapped method, and is also less sensitive to $L$ than the FM basis. However, the Laguerre basis is very bad for $\ell = 0$, competitive with the other methods for $\ell = 1$, and superior to the Chebyshev and Fourier schemes for $\ell = 12$. We have no explanation for this. However, the width of the modes depends on the 'principal quantum number' $n = j + \ell$ where $j$ is the mode number; $j$ is one for the lowest mode for each angular momentum $\ell$. Fig. 8 shows that the modes for higher $n$ are much wider and have smaller variations in scale than for $\ell = 0$ [20]. The wonder is not so much that the Laguerre basis has difficulties with $\ell = 0$, but rather that the other basis sets handle the disparity between the very narrow ground state and the much wider excited states so well.

A curious feature is that all methods display some surprisingly tall but narrow secondary peaks. For a narrow range of $L$ apparently outside the broad optimum range for a given method, the number of "good" eigenvalues suddenly rise to seven or ten. We have no good theoretical explanation, but the secondary peaks suggest that the spacing between eigenvalues is more accurate than the eigenvalues themselves.

Fig. 7(bottom) shows that spectral methods are not restricted to low angular momentum, but work just fine for $\ell = 12$. In contrast to $\ell = 0$, however, the Laguerre basis is the best. Both the Laguerre and rational Chebyshev bases are less sensitive to $L$ than the Fourier-mapped method.

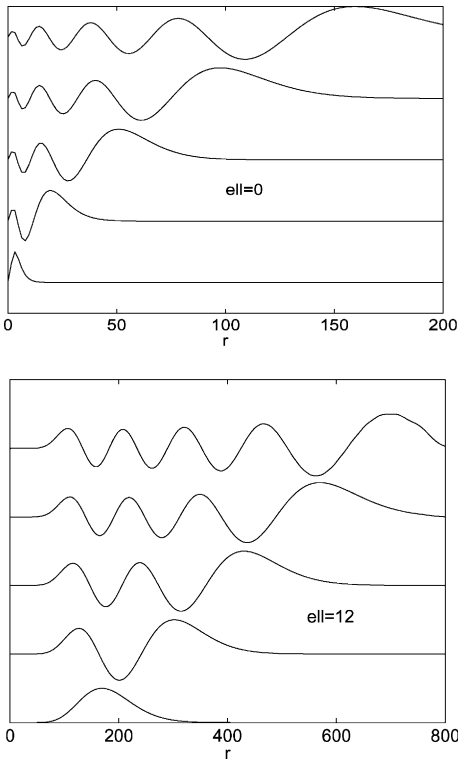


Fig. 8. A graph of the lowest, third-lowest, fifth-lowest, seventh-lowest and ninth-lowest eigenmodes for lithium for $\ell = 0$ (top) and $\ell = 12$ (bottom). The ground state is the lowest graph in each panel. Note that the scale for $\ell = 12$ is four times larger than for $\ell = 0$ because the modes are much wider for the higher principal quantum number.

## 9. Eigenfunction errors

The errors in the wavefunctions obviously follow the errors in the eigenvalues, so we will not make detailed comparisons between basis functions. Instead, Fig. 9 shows that it is straightforward to obtain high accuracy for lithium wavefunctions for $\ell = 0$–12. Laguerre functions were used for the illustrated computations, but similarly good results are obtained with our other basis sets.

As noted earlier, the optimum $L$ varies with the mode number. One can compute very high order lithium wavefunctions by shifting to a larger scaling/map parameter $L$ (not illustrated).

## 10. Optimizing the map or scale parameter

If the set of functions $\phi_j(r)$ is a basis set for the semi-infinite domain, then so also is $\phi_j(r/L)$ where $L$ is an arbitrary positive constant. It follows that for all basis sets for an unbounded interval, not merely the three compared here, there is a need to choose a scale parameter or map parameter $L$ that adjusts the width of the basis functions to (roughly) the width of the solution.

There is some theory for making this choice as outlined in [8–10,12]. The strategy is to apply the method of steepest descents to evaluate the usual spectral coefficient integrals in the limit that degree tends to

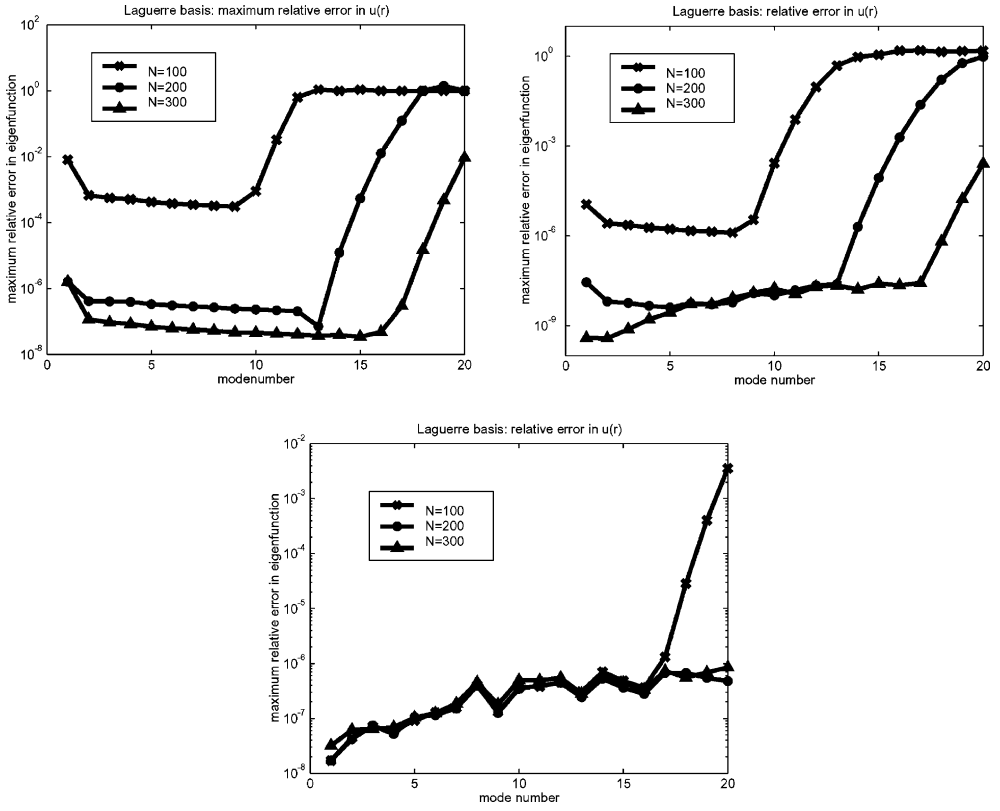


Fig. 9. Relative errors in the eigenfunctions of lithium using the Laguerre basis, computed by comparison to an "exact" solution using 450 basis functions. Upper left: $\ell = 0$, $L = 1$. Upper right: $\ell = 1$ with $L = 1$. Bottom: $\ell = 12$ with the Laguerre map parameter increased to $L = 6$.

infinity for a class of simple model functions, such as exponentials or functions with simple poles. The choice of $L$ that is best for these model functions is also near-optimum for functions that have similar decay rates as $r \to \infty$, or poles in similar locations. Although the predictive formulas are simple, it is not too easy

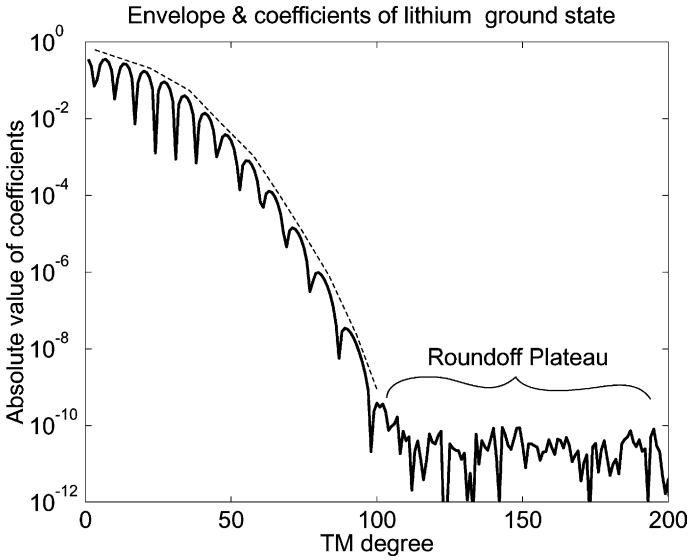


Fig. 10. The solid curve connects the absolute values of the spectral coefficients for a typical case. The dashed curve is the envelope. The coefficients $a_j$ stop decreasing and level off for sufficiently large $j$ because of roundoff error; the "roundoff plateau" where the coefficients are essentially random numbers is marked by the bracket. The point where the envelope intersects the roundoff error is (roughly!) the magnitude of the error.

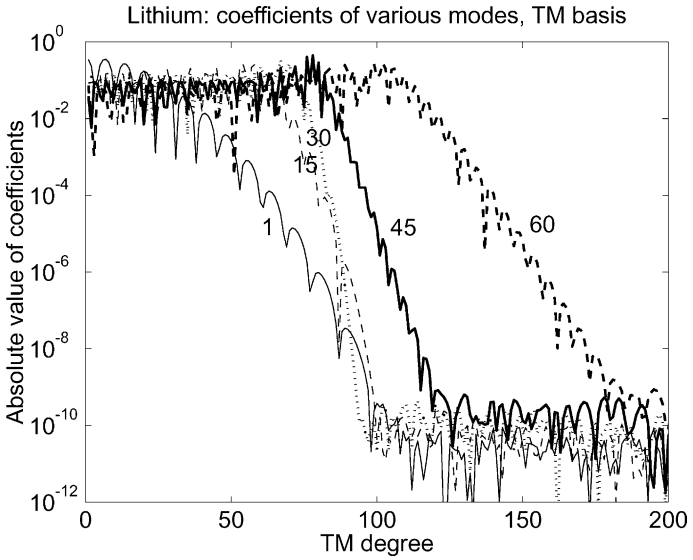


Fig. 11. Coefficients of seven selected eigenmodes of lithium, $\ell = 12$, in the TM basis. The mode labelled 1 is the lowest for this angular momentum (the most rapidly convergent series). The other modes are the 15th, 30th, 45th and 60th. The coefficients do not decrease below about $10^{-10}$ because the "roundoff plateau" is reached. Because the coefficients do decrease to such a small magnitude, it is likely that eigenvalues and eigenfunctions are accurate to eight or nine decimal places.

to effectively apply the theory because it is difficult to match an unknown solution with an appropriate model.

A good empirical strategy is to simply solve the problem and look at the spectral coefficients, plotted as absolute values on a log-linear plot, for several different values of $L$. The rational Chebyshev functions, for example, are the images of cosine functions under a change of coordinate, so obviously $|\mathrm{TM}_j(r;L)| \leqslant 1$ for all $r$ and $L$. This implies that the magnitude of the $j$th coefficient, $|a_j|$, is also a tight bound on the magnitude of the term, $|a_j \mathrm{TM}_j(r;L)|$.

Obviously, if the magnitudes of the coefficients (and therefore terms) are rapidly decreasing, the spectral series is accurate. One can be more quantitative: as explained in [14] (Chapter 2), the exponential rate of convergence implies that the error in truncating a spectral series after the $N$th term is roughly the same order of magnitude as the last computed coefficient $a_N$.

For expansions on an unbounded interval, the spectral coefficients seem to almost almost always oscillate in degree (as well as decay), but one can usually bound the coefficients from above by a straight line, or near-straight curve, which is called the "envelope". For oscillating-and-decaying series, the error estimate is the magnitude of the *envelope* at the truncation limit. Figs. 10 and 11 illustrate the envelope and also the flattening of the coefficients ("roundoff plateau") that occurs when the coefficients have decayed a limit set by roundoff error.

## 11. Spurious eigenvalues and convergence testing

As explained in Chapter 7 of [14] and also in [13] and other references cited there, matrix eigenvalue methods, when applied to a discretization of a differential equation, invariably generate many eigenvalues which are poor approximations to those of the differential equation. It is therefore always necessary to compare the calculated eigenvalues for two different truncations $N$, and to trust only those eigenvalues which are approximately independent of the truncation.

Most of the inaccurate or "spurious" eigenvalues are the larger numerical values, corresponding to high order eigenmodes that are inaccurately resolved by $N$-point discretization. However, for the $\ell = 0$ state of lithium with the Laguerre, there was a phony eigenvalue that was the *smallest* numerical eigenvalue. In other problems, such as Laplace's tidal equations, the spurious eigenvalues are interlaced with accurate, converged eigenvalues in a complicated way. The convergence-testing therefore often (but not always) needs to be between a pair of eigenvalues in two calculations that most closely resemble one another, and not merely between the smallest eigenvalue with $N = N_1$ with the smallest eigenvalue calculated with $N_2$ points [13].

## 12. Summary

The mapped Fourier-sine method of Fattal et al. is very accurate and has been used widely in quantum dynamics. However, the mapped Fourier scheme introduces a weak singularity at $r = 0$. This singularity is unnecessary. Both the Laguerre and rational Chebyshev bases give similar accuracy without inducing a singularity at $r = 0$, and the latter basis can, like the mapped Fourier-sine basis, be manipulated by means of the Fast Fourier Transform.

As a method of domain truncation, the number of accurate eigenvalues computed by the mapped Fourier-sine method does not increase with $N$ for all $N$. Instead, the error reaches a fixed plateau that depends only on the domain size $L$. The Laguerre and rational Chebyshev methods converge to zero error, in contrast, in the limit $N \to \infty$ for fixed $L$.

Because the total error of the mapped Fourier method is the sum of two separate errors, a domain truncation error $E_{\mathrm{D}}(L)$ and a series truncation error $E_{\mathrm{T}}(N)$, the total error is not an analytic function of $L$

for fixed $N$, but rather has a pointed cusp shape. Therefore, the mapped Fourier-sine method is more sensitive to the domain or scaling parameter $L$ than are the competing algorithms described here.

Because the grid spacing near $r = 0$ is so small, the mapped Fourier-sine algorithm is very costly when combined with explicit time-marching: the dense grid requires a very short time step.

We show that pseudospectral methods using a basis of Laguerre functions or rational Chebyshev functions are equally accurate or superior. The latter basis can be applied to time-dependent problems with the aid of the FFT like the mapped Fourier-sine scheme, but the Chebyshev basis allows a much longer time step for explicit time-marching schemes.

We have introduced a new species of rational Chebyshev functions, denoted $\mathrm{TM}_j$, which are associated with a grid that is more uniform for large $r$ than that of the older $\mathrm{TL}_j$ functions. At least for the hydrogen atom, this results in about a third again as many accurate eigenvalues for a given $N$.

However, the quest for better mapped-Fourier basis sets is open-ended. Some successful experiments for $x \in [-\infty, \infty]$ are described in [12,15,16]. Borisov [5], Lemoine [21] and Nest and Meyer [23] have made improvements for the semi-infinite interval, but all employ a sine basis with an extension-induced singularity at $r = 0$. There are better options.

## Acknowledgements

Supported by NSF Grant OCE9986368. C.R. gratefully acknowledges support from the NSF FOCUS Center. C.R. thanks Ronnie Kosloff for introducing her to the mapped-Fourier method, and Eyal Fattal for his programs and many helpful communications. We thank two reviewers and Thomas Heim for helpful comments.

## References

[1] M. Abramowitz, I.A. Stegun, Handbook of Mathematical Functions, Dover, New York, 1965.
[2] K. Banerjee, Hermite function solution of quantum anharmonic oscillator, Proc. R. Soc. Lond. A 364 (1978) 264.
[3] K. Banerjee, S.P. Bhatnagar, V. Choudhury, S.S. Kanwal, Anharmonic–oscillator, Proc. R. Soc. Lond. A 360 (1978) 575.
[4] J.N. Bardsley, Case Stud. Atom. Phys. 4 (1974) 302.
[5] A.G. Borisov, Solution of the radial Schrödinger equation in cylindrical and spherical coordinates by mapped Fourier transform algorithms, J. Chem. Phys. 114 (2001) 7770.
[6] J.P. Boyd, Spectral and pseudospectral methods for eigenvalue and nonseparable boundary value problems, Mon. Weather Rev. 106 (1978) 1192.
[7] J.P. Boyd, The choice of spectral functions on a sphere for boundary and eigenvalue problems: a comparison of Chebyshev, Fourier, and Associated expansions, Mon. Weather Rev. 106 (1978) 1184.
[8] J.P. Boyd, The optimization of convergence for Chebyshev polynomial methods in an unbounded domain, J. Comp. Phys. 45 (1982) 43.
[9] J.P. Boyd, Orthogonal rational functions on a semi-infinite interval, J. Comp. Phys. 70 (1987) 63.
[10] J.P. Boyd, Spectral methods using rational basis functions on an infinite interval, J. Comp. Phys. 69 (1987) 112.
[11] J.P. Boyd, Chebyshev domain truncation is inferior to Fourier domain truncation for solving problems on an infinite interval, J. Sci. Comp. 3 (1988) 109.
[12] J.P. Boyd, The rate of convergence of Fourier coefficients for entire functions of infinite order with application to the Weideman–Cloot sinh-Mapping for pseudospectral computations on an infinite interval, J. Comp. Phys. 110 (1994) 360.
[13] J.P. Boyd, Traps and snares in eigenvalue calculations with application to pseudospectral computations of ocean tides in a basin bounded by meridians, J. Comp. Phys. 126 (1996) 11;
Corrigendum 136 (1997) 227.
[14] J.P. Boyd, Chebyshev and Fourier Spectral Methods, second ed., Dover, Mineola, NY, 2001.
[15] A. Cloot, J.A.C. Weideman, Spectral methods and mappings for evolution equations on the infinite line, Comput. Meth. Appl. Mech. Eng. 80 (1990) 467.
[16] A. Cloot, J.A.C. Weideman, An adaptive algorithm for spectral computations on unbounded domains, J. Comput. Phys. 102 (1992) 398.

[17] P.J. Davis, P. Rabinowitz, Methods of Numerical Integration, second ed., Academic Press, Boston, 1984.
[18] A. Falqués, V. Iranzo, Edge waves on a longshore shear flow, Phys. Fluids 4 (1992) 2169.
[19] E. Fattal, R. Baer, R. Kosloff, Phase space approach for optimizing grid representations: the mapped Fourier method, Phys. Rev. E 53 (1996) 1217.
[20] H. Friedrich, Theoretical Atomic Physics, Springer, New York, 1990.
[21] D. Lemoine, Optimized grid representations in curvilinear coordinates: the mapped sine Fourier method, Chem. Phys. Lett. 320 (2000) 492.
[22] S.-H. Lin, R.T. Pierrehumbert, Does Ekman friction suppress baroclinic instability?, J. Atmos. Sci. 45 (1988) 2920.
[23] M. Nest, H.-D. Meyer, Improving the mapping mechanism of the mapped Fourier method, Chem. Phys. Lett. 352 (2002) 486.
[24] R.E. Robson, A. Prytz, The discrete ordinate/pseudo-spectral method: review and application from a physicist's perspective, Austral. J. Phys. 46 (1993) 465.
[25] Tao Tang, The Hermite spectral method for Gaussian-type functions, SIAM J. Sci. Comput. 14 (1993) 594.
[26] J.A.C. Weideman, S.C. Reddy, A MATLAB differentiation matrix suite, ACM Trans. Math. Software 26 (2000) 465.